GEOPHYSICAL RESEARCH LETTERS, VOL. 22, NO. 17, PAGES 2417-2420, SEPTEMBER 1, 1995

Calar Alto observations of Shoemaker Levy 9: Characteristics of the H and L impacts

D.P. Hamilton,[1] T.M. Herbst,[2] A. Richichi,[2] H. Böhnhardt,[3] and J.L. Ortiz[4]

Abstract. We describe data obtained at Calar Alto's 3.5-meter and 2.2-meter telescopes during the impacts of SL9 fragments H and L with Jupiter. Both the H and L impact lightcurves display three major features which we call 1) the first precursor, 2) the second precursor, and 3) the main event. The peak of the first precursor occurs before the onset of the Galileo PPR signal for each impact. We identify these three features with 1) the bolide entry into the jovian atmosphere, 2) the rising impact fireball, and 3) reimpacting ejecta. We also identify faint spots that appear near the H and L impact sites just before the respective events and suggest that the pre-L spot was caused by the J fragment which vanished in December 1993.

Introduction

During the Shoemaker-Levy 9 impacts on Jupiter, the Calar Alto 3.5-meter telescope was equipped with the MAGIC infrared camera which contains a NICMOS3 256 square detector array. The instrument is sensitive to near infrared wavelengths between 1 and 2.5μm and is described in detail by Herbst *et al.* (1993). This paper and its companion (Herbst *et al.* 1995 - HHBO95) discuss the observations and initial analyses of the Calar Alto 3.5m data; here we focus on 2.3μm imaging during the H and L impacts. Our primary data products are lightcurves which show the brightness of the impact region as a function of time. Under ideal conditions (large telescope, clear skies, 2.3μm filter), infrared lightcurves of a bright impact show three distinct peaks. In the next three sections, we discuss each of these features in chronological order: the first precursor, the second precursor, and the main event. We conclude by investigating faint spots that appeared before each impact.

The First Precursor

The H and L events are the only clear detections of the first precursor evident in Calar Alto data. Additional impacts available to us were less optimal because of small absolute intensities (A and Q2), confusion with pre-existing impact scars (Q1 and Q2), and reduced sensitivity during daytime events (E and S) – see HHBO95. The first H precursor, which peaks at 19:31:45 in the second panel of Fig. 1, appears in four of our images. Despite the 20-second spacing of the frames, the signal clearly rises quickly and decays over a longer time.

The L counterpart is the large well-resolved peak at 22:16:41 in the lower panel of Fig. 1. The L images are spaced only 1.2s apart over much of the lightcurve, allowing the identification of many subtle features. After a 15-30s gradual rise, the signal jumps sharply to its peak in only 9.3s. This rise is followed by an abrupt 2.3s drop to a plateau where the signal holds relatively constant for at least 8s. Finally the slowly-fading first precursor is swamped by the onset of the second precursor. Gaps in the lightcurve are due to data storage and telescope movements.

The simplest explanation for the first precursor is that it is due to the descent of the incoming bolide and an accompanying train of dust and small fragments through the upper jovian atmosphere. The distinguishing features of the first precursor – its rapid rise and even sharper drop in intensity – are what we expect from a single object descending through an exponentially-increasing atmosphere. The rise corresponds to increasing thermal emission as the bolide descends, and the cutoff occurs when the optical depth along the direct line of sight exceeds unity - about 750km (H) and 600km (L) above the one-bar level.

After the meteor disappears behind Jupiter's limb, some signal is still visible. We attribute this to the heated meteor track rising and expanding into view and also, perhaps, to reflection off cometary dust. We believe that the gradual increase of the signal for 15-30s before the sharp rise must be due to smaller objects which preceded L since the fragment itself was well above Jupiter's atmosphere at that time.

Support for these ideas comes from comparison of our timing results with those of Galileo's Photopolarimeter Radiometer (PPR). In particular, we note that the earliest Galileo signal for L comes 16s after the sharp rise in the Calar Alto data and a full 7s after the peak (Table 1). Although the uncertainties for H are larger, we are confident that Calar Alto's first H signal also occurred before Galileo's. The 7s between Calar Alto's L peak and the onset of Galileo's signal corresponds to a reasonable bolide flight path of about 400km. In addition, the PPR signal was observed at a wavelength of 945nm over 40s for L and over 29s for H (Martin *et al.* 1994), periods of time in which the infrared signals from Calar Alto decreased in strength. These facts suggest that the Galileo signals are due to the initial stages of an expanding fireball hidden from terrestrial observers.

[1] Max-Planck-Institut für Kernphysik, Heidelberg, Germany
[2] Max-Planck-Institut für Astronomie, Heidelberg, Germany
[3] Universitats-Sternwarte, München, Germany
[4] Instituto de Astrofisica de Andalucia, CSIC, Granada, Spain

Paper number 95GL01738
0094-8534/95/95GL-01738$03.00

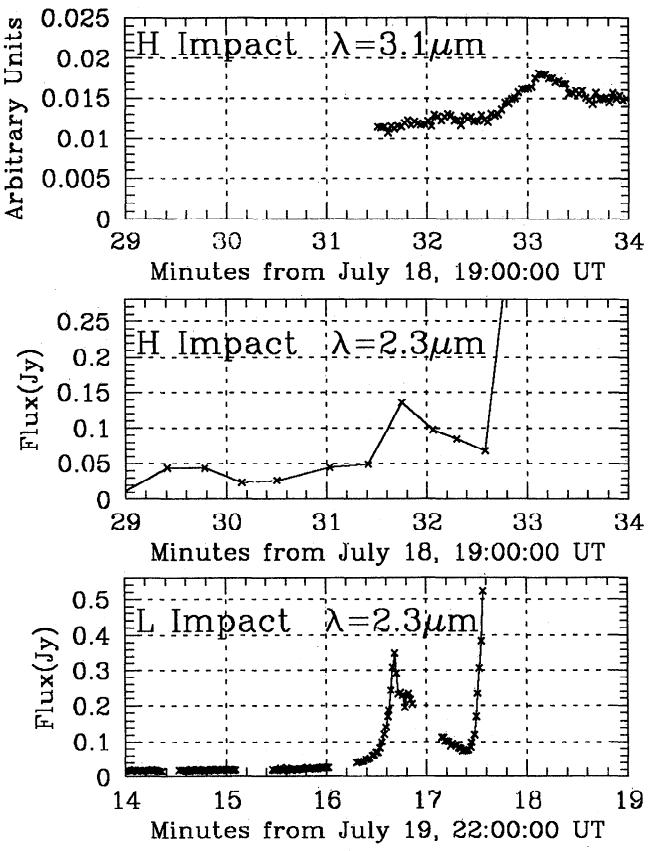

Figure 1. Lightcurves of the H and L first precursors. The first panel shows Calar Alto 2.2m fast photometer data and the remaining panels are derived from 3.5m MAGIC images. Crosses indicate exposure midpoints and all panels cover five minutes of time. The first precursor was not unambiguously detected by the photometer, but is clearly seen in the 3.5m data (peaks at 19:31:45 and 22:16:41). The second precursor begins about a minute later in all three panels. In each lightcurve, the nearly constant offset is background noise from Jupiter and the sky; these effects are larger for our near-sunset H observations. Accurate times for various features in this figure are given in Table 1.

The Second Precursor

The second precursor, starting less than a minute after the peak of the first, can be clearly seen in all panels of Figs. 1 and 2. In the 3.1μm photometer data (Fig. 2, panel 1), a minute-long peak is visible after which the signal rises slowly and continuously until the main event starts five minutes later. The 2.3μm data for both H and L, by contrast, show sharp rises to ledges of roughly constant intensity. A closer look at H (panel 2) reveals a rise to a peak and a slight drop one image later, followed by a slow rise and then a slow drop. These features are real and can be seen directly in the sequence of images. The initial peak for H at 2.3μm probably occurs between 19:33:13 and 19:33:26, about 10-20s later than the 19:33:07 peak in the 3.1μm lightcurve.

The differences between the two wavelengths is consistent with a hot bubble in the jovian atmosphere rising, spreading, and cooling in time. As the high-temperature fireball rises, signals at both wavelengths first increase due to geometry and cooling (Fig. 2). The earlier onset of the 3.1μm peak can be explained by the fact that the cooler outer layers of the rising bubble become visible to Earth-based observers first. The subsequent decrease in intensity between 19:35 and 19:37 at 2.3μm and the concurrent increase at 3.1μm indicates temperatures of about 900-1300K at this time.

Unfortunately our data for L's second precursor, visible on the right-hand side of Fig. 2's third panel, contains a data gap near 22:18 which was caused by saturation problems. After saturating, the signal decreased over 2-3 minutes and rose again to saturation at which point we switched to spectroscopy. The strength of the second precursor's peak is wavelength dependent; comparing our data to Keck (Graham *et al.* 1995) and Palomar (Nicholson *et al.* 1995) data, we see that peaks are sharper and brighter for longer wavelengths (our H data at 3.1μm and Palomar R data at 3.5μm and 4.5μm). In addition, at 2.3μm the peak is stronger for the large L impact (our data) than the smaller H and R impacts (our data and Keck data). Thus the feature is clearly dependent on wavelength and impact size; it probably also depends on the geometry of the impact.

The Main Event

The third and largest peak, the main event observed by Earth-based infrared instruments, can be seen in Fig. 2. The 3.1μm lightcurve shows that the main event has several distinct phases. The intensity rises sharply for two minutes, increases more slowly for 4min, drops for 4min, plateaus for 4min, and finally decreases again for 4min. In the 2.3μm H data, hints of some of these phases are evident, although the 10-min gap makes interpretations problematic. For instance, although there seems to be a slope change near 19:50 at 2.3μm, it is not as well pronounced as in the 3.1μm data. The maximum in the 3.1μm data occurs at 19:44:04 ± 9s and we estimate a peak time of between 19:44 and 19:45 from our 2.3μm lightcurve and from the behavior of spectra

Table 1. H and L Impact Timeline

Event	H Impact (July 18; 2.3μm)	L Impact (July 19; 2.3μm)
Mystery Spot	19:28:42 ± 11s	< 21:56:54
PC1 Start[1]	-	22:16:18 ± 03s
PC1 Sharp Rise	-	22:16:32 ± 03s
PC1 Peak	19:31:45 ± 20s	22:16:41 ± 03s
Galileo Start[2]	19:31:58 ± 01s	22:16:48 ± 01s
PC1 Drop	-	22:17:00 ± 09s
Galileo End[2]	19:32:27 ± 01s	22:17:28 ± 01s
PC2 Start	19:32:47 ± 12s	22:17:27 ± 03s
Main Start	19:37:27 ± 15s	-
Main Peak[3]	19:44:04 ± 09s	-
Main End	19:56:06 ± 30s	-

[1] PC1 = First Precursor; PC2 = Second Precursor
[2] Martin *et al.* 1995. PPR at 945nm.
[3] Fast photometer data at 3.1μm.

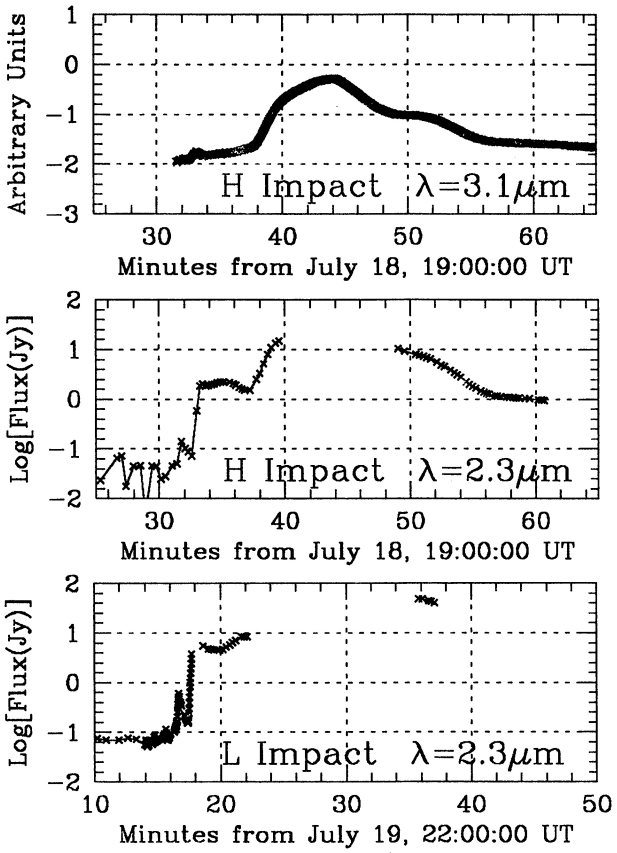

Figure 2. Full lightcurves for impacts H and L. As in Fig. 1, a panel of fast photometer data and two panels of MAGIC data are shown. All panels cover forty minutes and four decades of intensity. The faint first precursor, the ledge-like second precursor, and the bright main event are clearly evident. Large data gaps during the main events arise from spectral observations (HHBO95) which preclude accurate flux measurements.

taken during the 10-min gap. Although our L data on the main event are also sparse, they are in qualitative agreement with H.

Hubble images show that, as predicted by Zahnle and Mac Low (1994), material is ejected out along the bolide's incoming path (Hammel *et al.* 1995). With this in mind, we might expect several contributions to the main peaks of Fig. 2: thermal emission and reflected sunlight from in-flight ejecta, thermal emission from reimpacting ejecta, and direct emission from the impact site itself. During the infrared main events, Hubble images show bright plumes of material, well separated from Jupiter's visible limb, that rise and expand in time. These signals are interpreted as sunlight reflected from ballistic ejecta (Hammel *et al.* 1995). It is logical to assume that these plumes account for at least some of the signal detected by ground-based infrared instruments. Our spectral observations, however, are inconsistent with either reflected sunlight or blackbody thermal emission, showing instead distinct CO emission lines (HHBO95). Infrared main events, therefore, are dominated by non-equilibrium processes. The most likely mechanism is probably the release of kinetic energy during the collapse of the ejecta plume. The shoulder in the H lightcurve (Fig. 2, panels 1 and 2), which begins about 16 min after impact, provides an additional clue. The 16-min time difference is consistent both with the flight time of the high-velocity plume ejecta and with the time for the H impact site to rotate into view. Regardless of the cause, the fact that the shoulder appears prominently in 3.1μm data and only weakly in the 2.3μm data argues for relatively low temperatures.

The H and L Mystery Spots

Imaging data at 2.3μm for both the H and L impacts show very faint spots near the impact location on Jupiter's eastern limb well before even the first precursor. These spots are not apparent in the lightcurves, but are clearly visible in highly-stretched individual images. The pre-H spot is seen in the seven images taken between 19:28:42 and the first precursor maximum three minutes later (19:31:45). For L, the spot is visible in nearly 100 separate images between 21:56:54 and the first precursor (22:16:41). One of the sharper images of the L mystery spot is shown in Plate 1.

One possible explanation for the pre-H spot is that it is a remnant scar from fragment B which struck the planet about 4.10 jovian rotations (4 rotations + 57

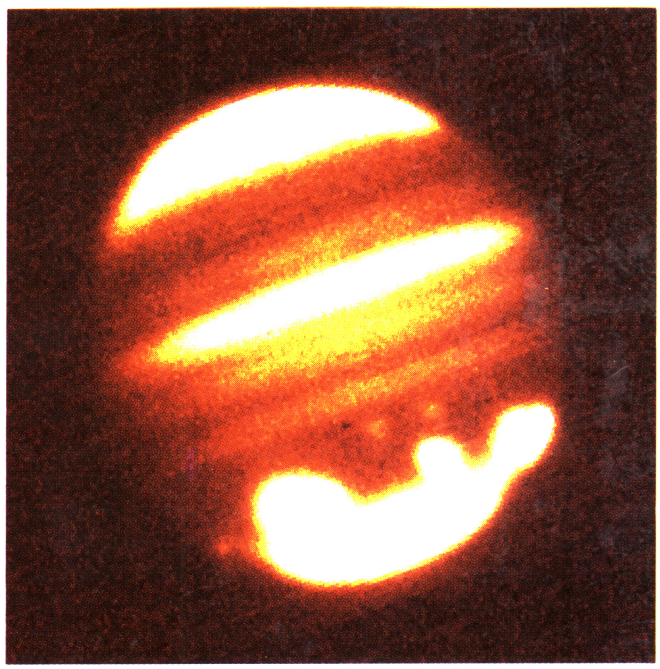

Plate 1. The L Mystery Spot. This highly-stretched 2.3μm image was taken on July 19, at 22:14:11 (see Fig. 1), well before the onset of the first precursor. The K, C, and A scars (left to right) and two of the faint temperate ovals (north of C) are visible below the bright equatorial stripes. The L mystery spot appears near the south-eastern limb, just to the left of the bright K complex. This spot was visible from 21:57, when observations at 2.3μm commenced, until it was overwhelmed 20min later by the much brighter first precursor.

minutes) before H. At the time of the H mystery spot, the B impact site should have been in sunlight and still near the limb. But since the B impact was very small (it was observed only by Keck and HST), it may not have left an appreciable scar. We believe that the pre-H spot was created by debris preceding the H fragment. Just prior to impact, the H dust coma was observed to be elongated along its direction of motion and three minutes of time corresponds to a reasonable extension of about 10,000km near Jupiter.

The L mystery spot, however, is unlikely to be directly associated with the L impact since the material would have to be widely separated to account for the 20-min time difference. We believe that this pre-L spot is caused by the impact of a separate small object. One likely candidate is the J fragment which faded from view in December 1993, more than six months before the impacts. The J fragment was predicted to strike Jupiter on July 19 at 02:40 ± 1:00 UT (Yeomans and Chodas 1994, public communication) and the mystery spot was visible in reflected sunlight when we began 2.3μm imaging on July 19 at 21:56:54. For the pre-L feature to be caused by J, the time separation needs to be at least 0.5 hours to bring J into sunlight plus two jovian rotations (9.925 hours) for a total of 20.35 hours. This scenario pushes the J impact back to at least 1:35 UT, about an hour earlier than the prediction. We find the alternative suggestion that a small previously-unknown fragment caused the mystery spot, less appealing. Unfortunately, our data cannot resolve the issue because the J impact and the subsequent appearances of its putative spot occurred at times unavailable for Calar Alto observations.

Conclusion

In this paper, we have presented arguments for the interpretation of infrared lightcurves obtained at Calar Alto and elsewhere. Although our interpretation is preliminary, the evidence for separate meteor, fireball and plume signatures is strong. Further analysis, and especially comparisons among diverse data sets, will be necessary to progress significantly in our understanding of these unique impacts.

Acknowledgments. The authors are grateful for the capable assistance of the Calar Alto staff during impact week. We thank Glenn Orton for a very detailed and helpful review. DPH acknowledges the support of an NSF/NATO postdoctoral fellowship.

References

Graham, J.R., I. dePater, J.G. Jernigan, M.C. Liu and M.E. Brown, W. M. Keck Telescope observations of the comet P/Shoemaker-Levy 9 fragment R Jupiter collision, *Science*, 267, 1320-1323, 1995.

Hammel, H.B., R.R. Beebe, A.P. Ingersoll, G.S. Orton, J.R. Mills, A.A. Simon, P. Chodas, J.T. Clarke, E. De Jong, T.E. Dowling, J. Harrington, L.F. Huber, E. Karkoschka, C.M. Santori, A. Toigo, D. Yeomans, R.A. West, Hubble Space Telescope imaging of Jupiter: Atmospheric phenomena created by the impact of comet Shoemaker-Levy 9, *Science*, 267, 1288-1296, 1995.

Herbst, T.M., D.P. Hamilton, H. Böhnhardt, J.L. Ortiz, Near Infrared Imaging and Spectroscopy of the SL-9 Impacts from Calar Alto, *GRL*, this issue, (HHBO95).

Herbst, T.M., S.V.W. Beckwith, Ch. Birk, S. Hippler, M.J. McCaughrean, F. Mannucci, and J. Wolf, in *Infrared Detectors and Instrumentation*, SPIE Technical Conference 1946, page 605, 1993.

Martin, T.Z., G.S. Orton, L.D. Travis, L.K. Tamppari, and I. Claypool, Observations of Shoemaker-Levy impacts by the Galileo Photopolarimeter Radiometer, *Science*, in press, 1995.

Nicholson, P.D., P.J. Gierasch, T.L. Hayward, C.A. McGhee, J.E. Moersch, S.W. Squyres, J. Van Cleve, K. Matthews, G. Neugebauer, D. Shupe, A. Weinberger, J.W. Miles and B.J. Conrath, Palomar observations of the R impact of comet Shoemaker-Levy 9: I. Light curves, *GRL*, this issue.

Zahnle K. and M.-M. Mac Low, The collision of Jupiter and comet Shoemaker-Levy 9, *Icarus*, 108, 1-17, 1994.

H. Böhnhardt, Universitats-Sternwarte, München, Germany.

D. P. Hamilton, T. M. Herbst, and A. Richichi, Max-Planck-Institut für Kernphysik, Postfach 103980, 69029, Heidelberg, Germany. (e-mail: hamilton@eu11.mpi-he.mpg.de)

J. L. Ortiz, Instituto de Astrofisica de Andalucia, CSIC, Granada, Spain.

(received December 12, 1994; revised April 2, 1995; accepted April 13, 1995.)